PROCEEDINGS OF SPIE

SPIEDigitalLibrary.org/conference-proceedings-of-spie

Using epoxy-based lithography to probe confinement effects on active nematics

Dimitrius A. Khaladj, Amanda J. Tan, Linda S. Hirst

Dimitrius A. Khaladj, Amanda J. Tan, Linda S. Hirst, "Using epoxy-based lithography to probe confinement effects on active nematics," Proc. SPIE 11092, Liquid Crystals XXIII, 110920F (29 August 2019); doi: 10.1117/12.2528602



Event: SPIE Organic Photonics + Electronics, 2019, San Diego, California, United States

Using epoxy-based lithography to probe confinement effects on active nematics

Dimitrius A. Khaladj, Amanda J. Tan and Linda S. Hirst* Dept. of Physics, University of California, Merced, 5200 N. Lake Rd., Merced, CA USA 95343

ABSTRACT

Active nematics are out-of-equilibrium liquid crystal fluids composed of rod-like subunits, which can generate large-scale, self-driven flows. In this emerging field of active nematics, new methods are needed to investigate and potentially control phase structure and dynamics. The use of complex engineered surfaces using microfabrication is an excellent way to control local orientation directors, taking advantage of the interplay between surface curvatures and topological defects. Epoxy-based lithography represents a simple and appealing approach, using low cost, minimal materials and a time efficient process. In this manuscript, we discuss methods for optimized fabrication protocols using negative and positive tone epoxy-based photoresists to create microfluidic devices for active matter. Arrays of curved objects and submerged topographies can be used to generate a variety of liquid crystal defect configurations not typically observed on unconfined planar surfaces.

Keywords: Active matter, nematic, SU8, microtubule, topological defect, molecular motors

1. INTRODUCTION

Active nematics have recently risen to prominence in the field of soft condensed matter and one of the most interesting examples is the recently developed biopolymer-based active nematic formed from bundled microtubule filaments in the presence of cross-linking kinesin motor clusters [1]. Active nematics must consist of energy-driven anisotropic elements to carry out their collective molecular motion. In such a phase defects can spontaneously arise, move around each other, annihilate and reform. In this case the biopolymers are driven by the action of motor proteins powered by ATP hydrolysis. A number of experimental methods have already been developed using the bundled microtubule framework [2-5]. Furthermore, theoretical and computational models have already been reported describing defect dynamics, pattern formation, and methods to mathematically characterize the system [5-9]. With the use of microfluidics, we aim to expand and build on Sanchez' framework by creating complex surfaces and to observe their influence on defect behavior. The incorporation of new surfaces or immiscible boundaries adds more complexity to an active nematic system [9,10]. We will discuss methods to expand more on the effects of anchoring on bundled microtubule active nematics with the creation of fabricated boundaries.

Molecular anchoring in a liquid crystal phase refers to the imposed orientation of the liquid crystal director, n with respect to a boundary, surface or interface [11]. When a confining surface induces a particular anchoring condition, there may be frustration between the intrinsic molecular ordering of the phase and the tendency of the phase to align with the container boundary. This interplay of steric molecular interactions and elastic energy minimization can lead to topological defects depending on the specific geometry of the container [11]. In the active materials first reported by Sanchez et al [1], we see planar microtubule anchoring since the active nematic is confined at the flat two-dimensional boundary between oil and aqueous fluid layers (Figure 1). In a passive nematic phase in two dimensions, without confining boundaries, no defects are topologically required, however they may occur spontaneously. In an active nematic we see the emergence of pairs of topological defects (+1/2 and -1/2) that braid around one another, continually annihilating and reforming (Figure 1b). This is the most simple example of how anchoring can be used to promote an active phase and defect formation.

Figure 2 shows a cartoon representation of the molecular system, in which the microtubule filaments are coupled together by kinesin motor protein clusters via a streptavidin linkage. The motor pairs walk in opposing directions, producing a local shearing motion. Bundles are stabilized with polyethylene glycol (PEG) via depletion forces [1].

*lhirst@ucmerced.edu

Liquid Crystals XXIII, edited by lam Choon Khoo, Proc. of SPIE Vol. 11092, 110920F · © 2019 SPIE · CCC code: 0277-786X/19/\$21 · doi: 10.1117/12.2528602

In a typical experiment, the suspension is confined between two immiscible fluids, water and oil, to form a continuous nematic phase across the fluid-fluid interface, where no obstacles are present that may perturb or influence flow. In this paper, we explore methods by which we can create novel surfaces and topologies to influence flow patterns and defect formation in the active nematic (Figure 2b). Beyond two-dimensional fluid-fluid confinement, hard boundaries can be designed via microfabrication to influence defect dynamics.

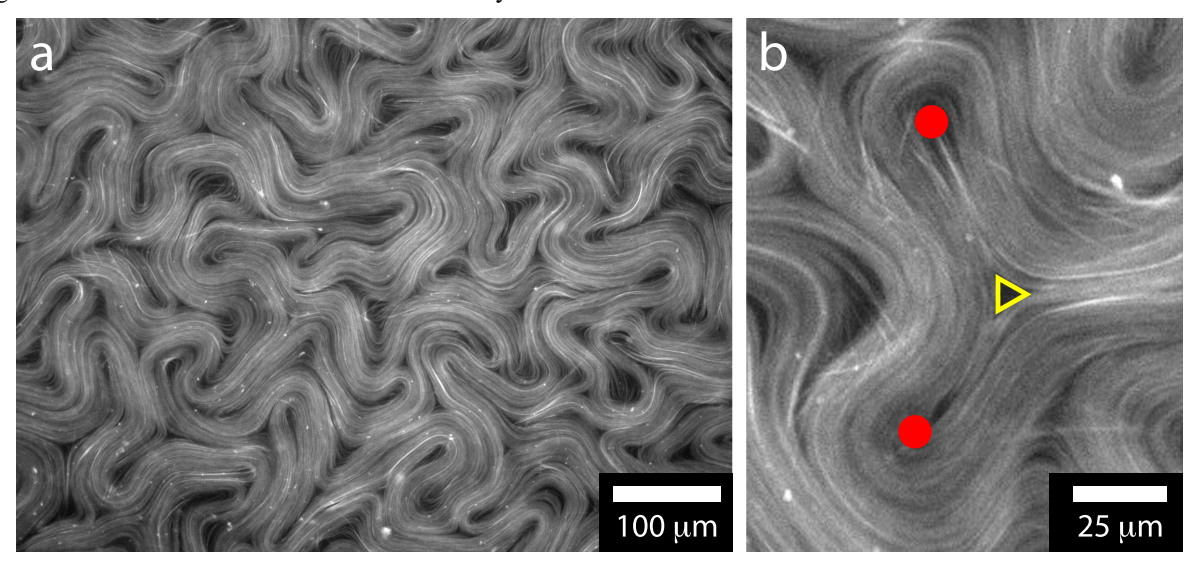


Figure 1. Fluorescence microscope images of a microtubule/kinesin two-dimensionally confined active nematic phase as used in this paper. (a) A large area of active nematic flow, (b) close-up view of three topological defects in the flow, $\pm 1/2$ (red circles) and $\pm 1/2$ (yellow triangle).

Photolithography is the primary method for the fabrication of transistors in the semi-conductor industry and has also been effectively used in a plethora of bio-related applications, for example, in tissue engineering and micro-fluidics [12]. This has been promising in the construction of novel surface topographies and micro-environments to observe biological fluids and control flows and processes. The investigation of active flows in micro-fluidic environments (with geometrical confinement), is in its infancy, however some fascinating results have already arisen. In a recent paper, Opathalage et al. [2] confined an active nematic to cylindrical wells of different sizes. This setup demonstrated the emergence of spontaneous circular periodic flows with increased confinement. At large radii the material behaved similarly to that in open unconfined systems, including the emergence of chaotic flows and continuous defect braiding [6]. At the smallest radii in [2], they saw that a single circular flow emerged. Similar behaviors have also been reported in bacterial suspensions and for actin-based system influenced by sidewall anchoring [13,14]. In these cases, cylindrical wells contribute to bundle deformation in a biased direction and extensile motion generates a circular flow along the container boundary.

In another interesting direction, straight walled trenches were employed as a confinement strategy by Jerome et al. [11] in passive nematics, and then, recently for active nematics [3,4]. In this linear configuration, the bundled active nematic is confined to rectangular microfluidic channels with widths between $90\mu m$ to $120\mu m$. Defects are observed to braid around each other in a distinct pattern and also concentrate in specific regions within the channel. In particular, the authors noted that -1/2 defects tend to localize on the sidewalls of the channel and +1/2 defects tend to localize midway through the trench [3,4]. Furthermore, +1/2 defects were observed to annihilate when approaching the sidewall; this is the caused by the large concentration of -1/2 defects in this region of the device.

It is clear that confining geometries can have a significant impact on the motion of topological defects in active nematics. The behaviors observed so far may just be the beginning of our ability to control and manipulate active materials. In this paper we report a strategy to design and fabricate confining structures for active nematics including circular wells and pillars and trenches from glassy polymers.

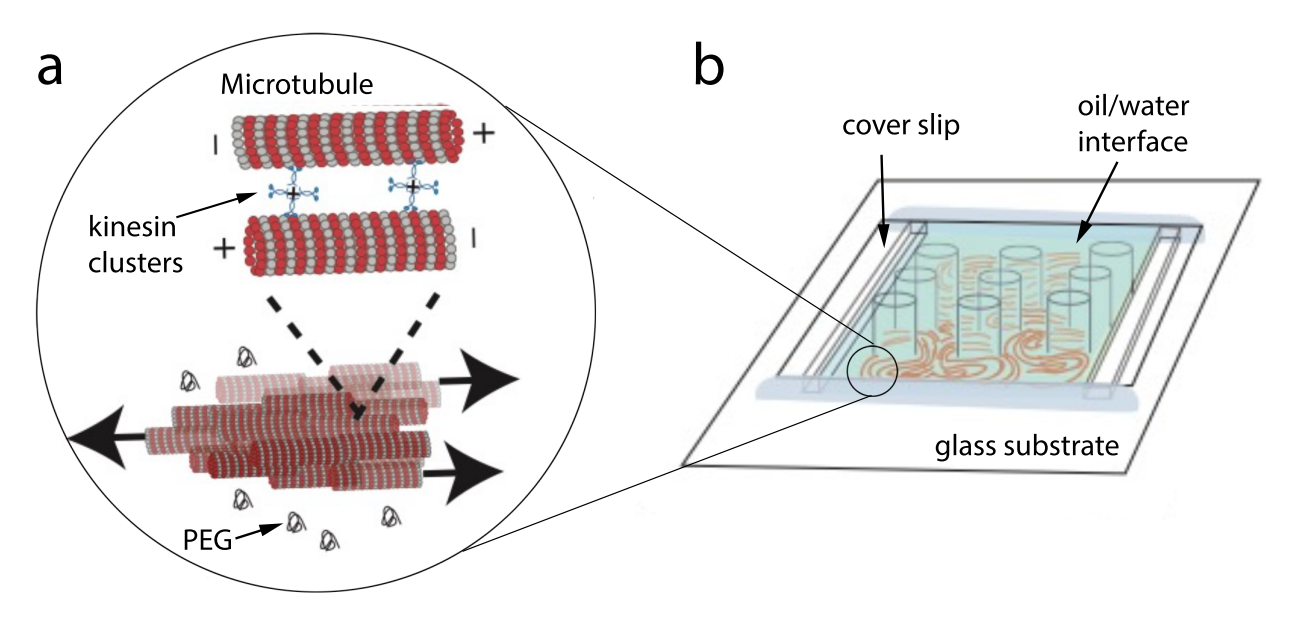


Figure 2. Schematics of the experimental system and flow cell including a) a detailed visualization of the protein construct including bundled microtubules connected by kinesin motor clusters and b) the flow cell geometry including microfabricated SU8 pillars.

2. METHODS

2.1 Formation of the Active Nematic

The microtubule/kinesin-based active nematic is formed by previously described methods [1]. 10µl aliquots of an active premixture containing biotin-labeled K401 kinesin motors, streptavidin, PKLDH and phosphoenol pyruvate (PEP) (an ATP regenerating system), an antioxidant solution to prevent photobleaching containing 6.65mM DTT, 4mg/ml glucose, 0.27 mg/ml glucose oxidase, 47µg/ml catalase and 2mM Trolox, and 6% (w/v) 20kD polyethylene glycol (PEG) in M2B buffer (80mM PIPES pH 6.8, 2mM MgCl₂, and 1mM EGTA) are previously prepared as described in [1, 6]. 1mM ATP (final concentration) is added to the premixture. 2µl of 6mg/ml (3%) Alexa Fluor 647 labeled GMPCPP microtubules are added to the premixture (for a final concentration of 1mg/ml). For fluorescence imaging, microtubules are fluorescently labelled with Alexa Fluor 647 [1]. This system forms a 3D, unconfined, active microtubule network. Streptavidin can bind up to four biotin-labeled kinesin molecules (Figure 2) and when microtubules of opposing polarities align parallel to each other, the kinesin molecules oriented at 180° to each other walk in opposite directions along those neighboring microtubules. As the kinesins walk, the filaments produce an extensile motion driven by ATP hydrolysis. We used an ATP concentration at saturation (i.e. the local microtubule extension speed was maximized).

To confine the active nematic at the oil/water interface, we follow a previously published procedure [1, 6]. We first create a flow cell made from the glass substrate with patterned structures, double-sided tape and a coverslip treated with a polyacrylamide brush (see Figure 2b). The polyacrylamide brush prevents excess protein binding to the coverslip. We flow in an oil/surfactant mixture (3M HFE7500 with 1.8% PFPE-PEG-PFPE (perfluoropolyether) surfactant) into the channel. Then, this mixture is exchanged with the active microtubule network. The ends of the flow cell are sealed using a UV-curable glue (RapidFix). The sample is then centrifuged in a swinging bucket rotor for 42 min at 300 rpm.

2.2 Photolithography

A simple schematic for a single-patterned fabricated structure is illustrated in figure 3. The photoresist is spun onto a substrate. The type of wafer depends on the application, but for our system, we use glass as a substrate for our structures. The resist is spun down creating a thin uniform coating onto the substrate where thickness depends on the speed in which the wafer/glass spins. There are two types of photoresist in lithography based on their tones, negative and positive. The tone depends on the photochemistry of the deposited film when exposed to 365nm of ultraviolet light. One of the properties of photoresists is their photosensitivity. When exposed to light (in this case 365nm), photoacid generators (PAGs) are released from within the film. The polymer and PAGs are suspended in a solvent, thus they are distributed evenly

throughout the exposed cross-section of the film. When heated, the acids effect the film's solubility. If the film is positive tone, the PAGs break up the polymer, changing it from insoluble to soluble in aqueous solution. If the film is a negative tone resist, the acid released from the PAGs causes crosslinking, producing a change from soluble to insoluble in aqueous solution.

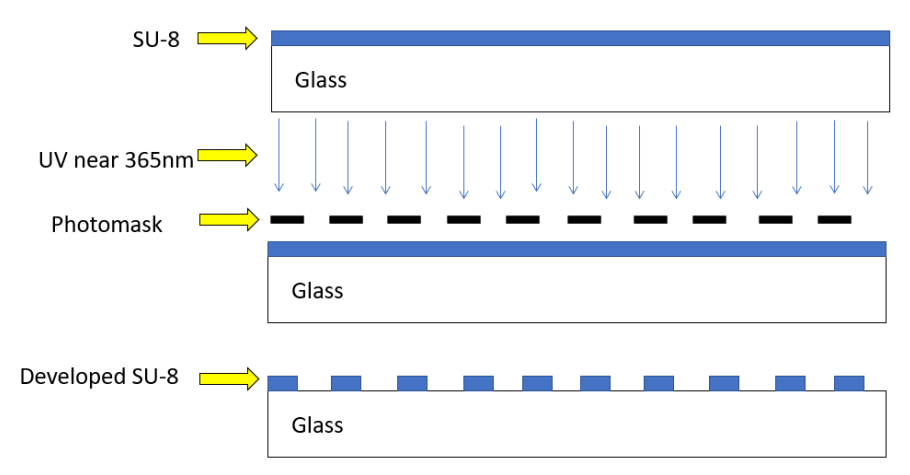


Figure 3. Flow diagram illustrating a single exposure process using a negative tone photoresist.

SU-8 (MicroChem Corp.) is an epoxy-based negative tone photoresist that can create thin plastic substrates upon exposure and development. It has a wide range of applications in bio-medical devices, cell encapsulation and microfluidics due to its biocompatibility. SU-8 comprises epoxy-based monomers suspended in solvent and PAGs. Upon exposure to ultraviolet (UV) light, the PAGs release acids which serve as a catalyst for the cross-linking reaction. Once the PAGs are released, the film is exposed to a 95°C post exposure bake (PEB) and the acids induce cross-linking of epoxy groups in the film.

The PEB facilitates cross-linking within the SU-8 layer. Heating the film above its glass transition temperature ($T_g = 55^{\circ}$ C) increases the molecular motion of the monomers and PAGs resulting in an increased cross-linking rate. It is important to emphasize that extensive cross-linking affects the mechanical properties of the film as the network will become stiffer. During the development step, the exposed regions remain on the substrate as the cross-linking affects the films solubility in that specific region.

Adhesion of SU-8 on a substrate is another important factor for device production. Substrate to film interaction, substrate cleanliness, film thickness and surface preparation must be considered prior to fabrication. The presence of impurities, moisture, and other residual coatings can greatly compromise adhesion resulting in leaks between the substrate-SU-8 interface which affects device performance and functionality [15]. Glass substrates are cleaned thoroughly in soap and water followed by sonication for 30 minutes in Acetone, methanol, ethanol then rinsed in nanopure water to ensure minimal presence of surface contaminants. To ensure that the surface is thoroughly clean, the surface is plasma treated with oxygen for 30 seconds. To ensure the removal of residual moisture, glass substrates are placed on a 200°C hotplate for 5 minutes and allowed to cool down for 5 minutes at room temperature.

It is worth noting that film thickness should be carefully considered when designing substrates. Thicker films tend to be highly stressed resulting in cracks, warping of the features and poor adhesion (Figure 4). For thicker resins such as SU-8 50, we used gradual cool downs to room temperature after the PEB and a hard bake at 150°C for 2 minutes post development. These steps greatly improved adhesion, resolution of the film pattern, and reduced cracking.

2.3 Fabrication protocol for thick 3-D SU-8 structures

A quarter-sized drop of SU-8 50 is deposited on a cleaned glass substrate, which is then spin coated at 2000 rpm for 45 s followed by a 10 min wait time. The substrate is then soft baked at 65°C on a hot plate for 12 minutes then at 95°C for 45 minutes. The substrate is subsequently removed from the hot plate and allowed to cool at room temperature for 10 min, then exposed to 365nm UV light (500 mJ cm⁻²). The film is rested for another 10 min then baked at 65°C for 5 min, then again at 95°C for 15 min. After the 15 min bake at 95°C, the hot plate is turned off and allowed to cool down to room temperature to avoid thermal shock on the film. The substrate is developed in SU-8 developer for 30 min with gentle agitations. Once developed, the residual SU-8 developer is rinsed away with isopropanol and de-ionized water then dried

with nitrogen gas. As a final step, the device is hard baked at 150°C for 2 min. Figure 5 shows two images of a finished device. An array of SU-8 pillars on a glass substrate incorporated into a flow channel. The channel can be sealed with a glass cover slide and fluids introduced into either end.

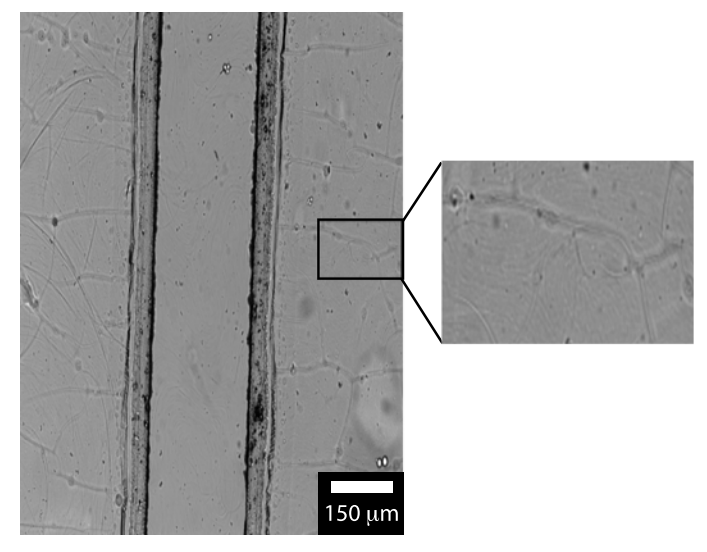


Figure 4. Bright field microscope image of a microfabricated thick SU-8 trench. The inset image highlights cracks in the polymerized surface due to rapid cooling.

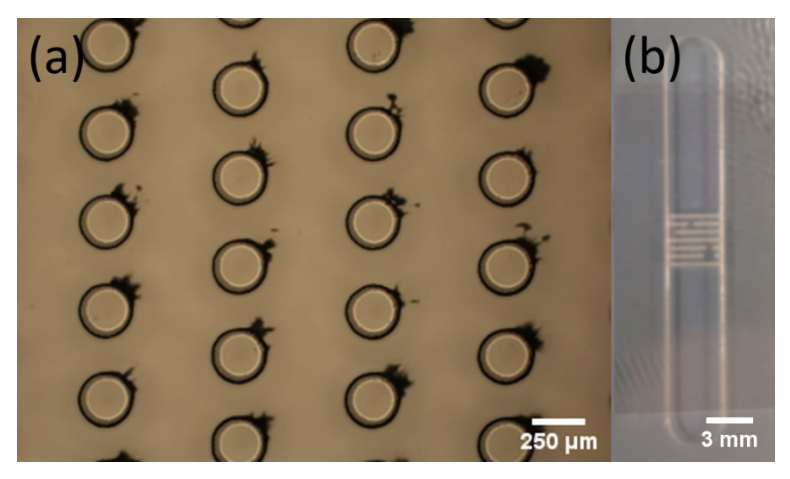


Figure 5. (a) Bright field microscope image of fabricated SU-8 pillars and (b) an overview image of the entire microfluidic device with the pillar array at the center. The vertical trench is used to introduce the active material to the pillars.

Figure 6 shows a diagram of the pillars with respect to the oil/water interface. Using this pillar system it is possible to produce curved fluid interfaces by tuning the spacing of the pillars where $h_{pillar} > h_{oil}$ (h_{pillar} is height of a pillar and h_{oil} is the height of the oil layer). SU-8 is coated with Aquapel resulting in a hydrophobic surface, and so the oil wets the pillar causing the oil layer to curve upwards. Such structures may be useful to investigate the behavior of active nematics on tunable curved interfaces, free from the influence of a hard substrate.

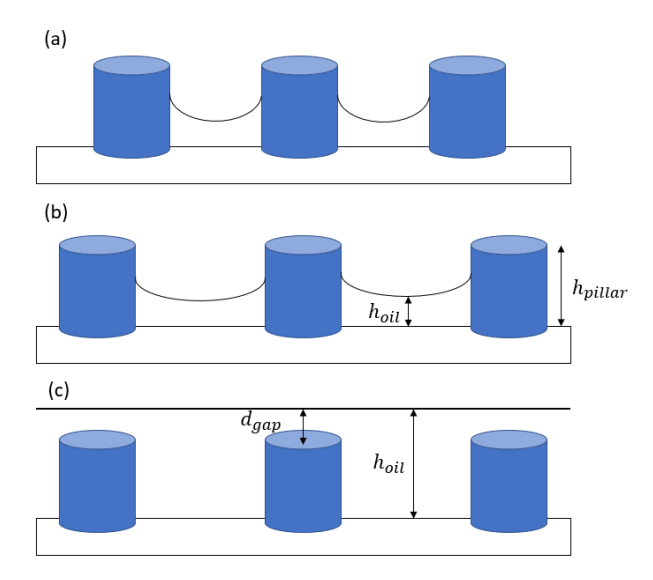


Figure 6. Illustration of the oil/water interfacial layer wetting fabricated pillars. (a) SU-8 pillars with a height greater than the thickness of the oil layer; the smaller separation distance results in high interfacial curvature at the oil/water boundary layer. (b) Similar configuration to (a) but larger separation distance between pillars resulting in a larger radius of curvature. (c) SU-8 pillars with a height less than the thickness of the oil layer, i.e. submerged in the oil layer.

3. RESULTS

3.1 Influence of SU-8 pillars on microtubule-kinesin active nematic

The goal of our research is to design and construct microfabricated surfaces in a transparent flow cell configuration that can be used to investigate the effects of confining geometries on active flows. Using the devices described above we demonstrate the effect of circular pillars in this section. The pillars act as circular boundaries within the active layer in the x-y plane, and wetting behavior of the oil/water interface on the pillars may also lead to additional curvature-based effects in the z-axis direction (into the page).

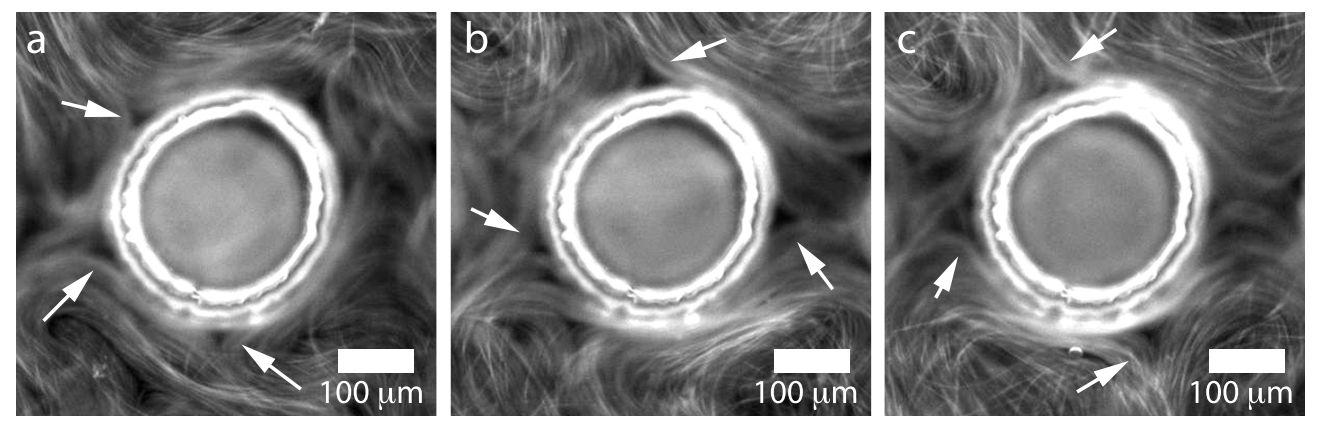


Figure 7. Fluorescence microscope images of active nematic surrounding an SU8 pillar. Snapshots are shown at a) t = 0 s, b) 113 s and c) 178 s. -1/2 defects (indicated by white arrows) can be seen to locate and persist at the pillar/fluid interface.

Figure 7 shows fluorescence microscope images of an active nematic flow surrounding a circular SU-8 pillar. Despite the expected planar anchoring for these pillars, we observed several -1/2 topological defects distributed around the pillars. These defect points tend to persist and remain somewhat immobile as the rest of the active layer flows around the pillars. This persistent defect configuration is similar to that seen recently in linear channels [3, 4] and it will be interesting to see how different shapes and sizes of pillars and their arrangements affect the persistence of defect points.

Until recently, investigation into active nematics was largely focused on flat interfaces, but by designing pillar arrays and channels with the right wetting properties, it may be possible to produce interesting curved interfaces between oil and water. For example, if $h_{pillar} > h_{oil}$, the oil layer wets the surface of the SU-8 pillar resulting in curvature of the oil/water interface (Figure 6). Pillars or different shapes can be fabricated with different separation distances, thus allowing us to tune the curvature of the interface.

The active nematic is also observed to have an affinity for regions where the pillars are present. The active network tends to concentrate near the pillars, rather than spread throughout the flow cell uniformly. We have observed the active nematic to concentrate and braid around the pillar arrays, whereas lower concentrations of the microtubule network are observed everywhere else. This attractive tendency could be due to curvature from the oil layer wetting the SU-8 structure. Once formed, the persistent motion around the pillars could be explained by the higher density of microtubule bundles in the confined region – i.e. the network prefers to stay together once a flow around the pillar is initiated as kinesin binding sites and other microtubules are more available near the pillars than in the unconfined region. To expand on these observations, pillars can be fabricated with different separation distances which will affect the radius of curvature between neighboring structures. To measure interfacial curvature, we can use confocal microscopy and determine the shape created as it may not be spherical.

In figure 8, active matter is seen to flow around several pillars and two interesting phenomena can be highlighted. The fluorescence image shows that in the narrow gaps between pillars the active nematic appears to go out of focus – it bends down out of plane in the z-direction. This effect is likely due to competition between anchoring conditions at the fluid interface (the microtubules tend to align with the interface) and the elastic cost of bending the microtubule bundles as defects try to pass through a narrow aperture. The active flows pass through the gaps between the pillars by escaping into the 3rd dimension, i.e. the z direction, possibly deforming the interface at that point and thus minimizing the bending energy cost. Secondly, defects between the rows of pillars appear to braid around each other in a manner similar to the silver braid reported recently [3,4,6], as if the network was confined to a thin trench. This effect also supports the idea that the bundles are to some extent repelled from the narrow apertures due to bending constraints, and thus the pillar array acts as a virtual channel.

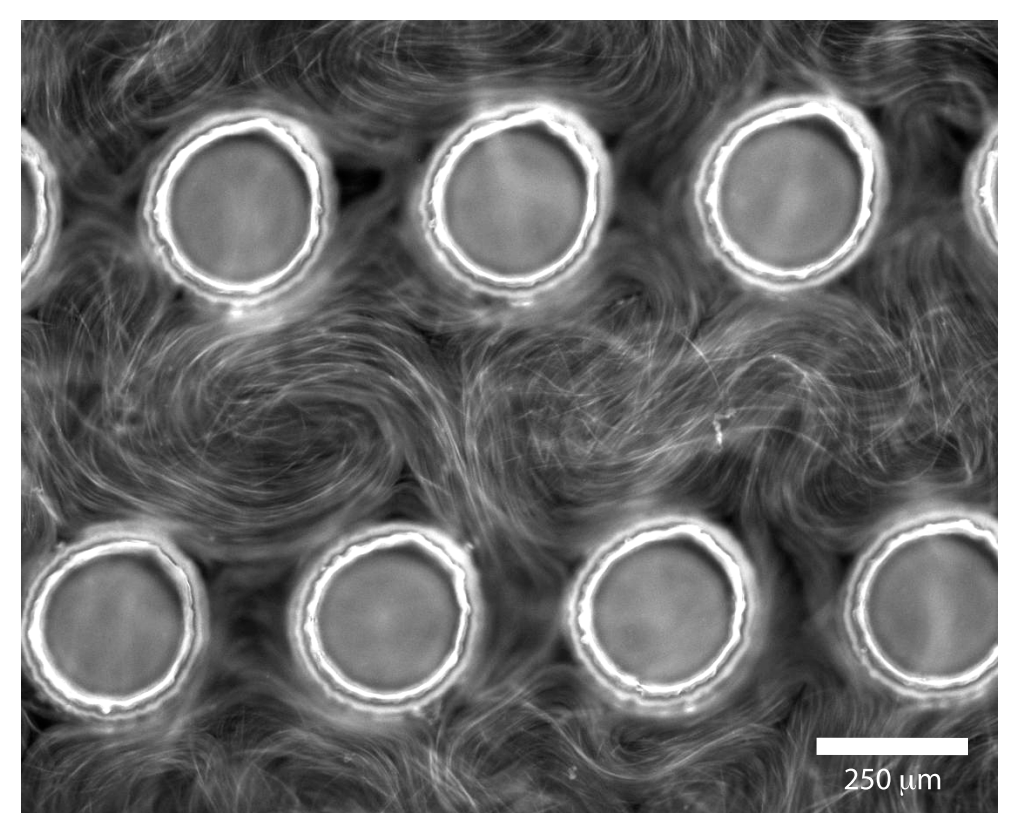


Figure 8. Bundled microtubule active nematic flows interacting with an SU-8 pillar array.

Finally, we have also made observations of the active nematic system under the condition $h_{pillar} < h_{oil}$ (see figure 6c) i.e the fabricated structures are submerged in the oil layer and the active matter moves in a continuous plane over the submerged structures. This setup appears to have some interesting consequences and preliminary results show that defect speeds are affected by the presence of the submerged structures. It will be interesting to investigate the relationship between defect dynamics and the separation distance between the active nematic and the top of a pillar, d_{gap} . Using the convenient SU-8 devices we have developed, it will be possible to perform these future experiments.

4. CONCLUSIONS

In this paper we report on methods to create active-nematic compatible microstructures using SU-8, a biocompatible glassy polymer formed using a negative-tone lithography process. The structures can be used to confine active material in a transparent flow cell ideal for bright field and fluorescence microscopy. Using these techniques various experimental configurations are envisioned, including pillar arrays and submerged structures. Using these simple tools it will be fascinating to explore the impact of different geometries on chaotic flows in active nematics.

5. ACKNOWLEDGEMENTS

Our group is grateful to Prof. Zvonimir Dogic for the generous contribution of microtubules and molecular motors and to Linnea Lemma for sample preparation. We would also like to thank Anand Gadre for useful discussions regarding fabrication techniques and problem solving. The authors acknowledge generous funding from the National Science Foundation, through several awards: DMR-1808926, NSF-CREST: Center for Cellular and Biomolecular Machines at UC Merced (HRD-1547848) and from the Brandeis Biomaterials facility MRSEC-1420382.

- [1] Sanchez, T., Chen, D. T. N., DeCamp, S. J., Heymann, M. & Dogic, Z. "Spontaneous motion in hierarchically assembled active matter," Nature 491, 431–434 (2012).
- [2] Opathalage, A., Norton, M. M., Juniper, M. P. N., Langeslay, B., Aghvami, S. A., Fraden, S., Dogic, Z. "Self-organized dynamics and the transition to turbulence of confined active nematic," Proc. Natl. Acad. Sci. 116(11), 4788-4797 (2019).
- [3] Hardouin, J., Hughes, R., Doostmohammadi, A., Laurent, J., Lopez-Leon, T., Yeomans, J. M., Ignes-Mullol, J., Sagues, F. "Reconfigurable flows and defect landscape of confined active nematics," under review. (2019).
- [4] Doostmohammadi A., Ignes-Mullol J., Yeomans J. M., Sagues F. "Active nematic," Nat Comm. 9:3246. (2018)
- [5] Shendruk, T. N., Doostmohammadi, A., Thijssen, K. Yeomans, J. M. "Dancing disclinations in confined active nematic," Soft Matter 13, 3853 (2017).
- [6] Tan, A. J., Roberts, E., Smith, S. A., Olvera, U. A., Arteaga, J., Fortini, S., Mitchell, K. A., Hirst. L. S. "Topological chaos in active nematic," Nat. Phys. In press (2019).
- [7] Maitra, A., Srivastava, P., Marchetti, M. C., Lintuvuori, J. S., Ramaswamy, S., Lenz, M. "A nonequilibrium force can stabilize 2D active nematic," Proc. Natl. Acad. Sci. 115(27), 6934-6939 (2018).
- [8] Shankar, S., Ramaswamy, S., Marchetti, M. C., Bowick. M. J. "Defect Unbinding in Active Nematic," Phys. Rev. Lett. 121, 108002 (2018).
- [9] Cui, Z., Su, J., Zeng, X. "Effects of Anchoring Boundary Conditions on Active Nematic," Current Nanoscience. 13(4) (2017)
- [10] Batista, V. M. O., Blow, M. L., Telo da Gama, M. M. "The effect of anchoring on the nematic flow in channels," Soft Matter 11, 4674–4685 (2015)
- [11] Jerome, B. "Surface effects and anchoring in liquid crystals," Rep Prog Phys. 54(3), 391-451 (1991).
- [12] Grenci, G., Bertocchi, C., Ravasio. A., "Integrating Microfabrication into Biological Investigations: the Benefits of Interdisciplinarity," Micromachines. 10(4), 252 (2019)
- [13] Wioland, H., Woodhouse, F. G., Dunkel, J., Kessler, J. O., Goldstein, R. E. "Confinement stabilizes a bacterial suspension into a spiral vortex," Phys. Rev. Lett. 110, 268102. (2013).
- [14] Tee, Y. H., Shemesh, T., Thiagarajan, V., Hariadi, R. F., Anderson, K. L., Page, C., Volkman, N., Hanein, D., Sivaramakrishnan, S., Kozlov, M. M., Bershadsky, A. D. "Cellular chirality arising from the self-organization of the actin cytoskeleton," Nat. Cell Biol. 17(4), 445-57 (2015).
- [15] Mitra, S. K., Chakraborty. S., [Microfluidics and Nanofluidics Handbook: Fabrication, Implementation, and Applications] CRC Press. Boca Raton. 231-262 (2012).